Genome-wide linkage identifies novel modifier loci of aganglionosis in the *Sox10^Dom* model of Hirschsprung disease

Sarah E. Owens[1], Karl W. Broman[2], Tim Wiltshire[3], J. Bradford Elmore[1], Kevin M. Bradley[1], Jeffrey R. Smith[1] and E. Michelle Southard-Smith[1],*

[1]Division of Genetic Medicine, Department of Medicine, Vanderbilt University School of Medicine, 529 Light Hall, 2215 Garland Avenue, Nashville, TN 37232-0275, USA, [2]Department of Biostatistics, Bloomberg School of Public Health, Johns Hopkins University, 615 N Wolfe Street, Baltimore, MD 21205-2179, USA and [3]Genomics Institute of the Novartis Research Foundation, 10675 John Jay Hopkins Drive, San Diego, CA 92121, USA

Hirschsprung disease (HSCR) is a complex disorder that exhibits incomplete penetrance and variable expressivity due to interactions among multiple susceptibility genes. Studies in HSCR families have identified *RET*-dependent modifiers for short-segment HSCR (S-HSCR), but epistatic effects in long-segment (L-HSCR) and syndromic cases have not been fully explained. *SOX10* mutations contribute to syndromic HSCR cases and *Sox10* alleles in mice exhibit aganglionosis and pigmentary anomalies typical of a subset of HSCR patients categorized as Waardenburg–Shah syndrome (WS4, OMIM 277580). *Sox10* mutant alleles in mice exhibit strain-dependent variation in penetrance and expressivity of aganglionic megacolon analogous to the variation observed in patients with aganglionosis. In this study, we focused on enteric ganglia deficits in *Sox10^Dom* mice and defined aganglionosis as a quantitative trait in *Sox10^Dom* intercross progeny to investigate the contribution of strain background to variation in enteric nervous system deficits. We observe that the phenotype of *Sox10^{Dom/+}* mutants ranges over a continuum from severe aganglionosis to no detectable phenotype in the gut. To systematically identify genes that modulate *Sox10*-dependent aganglionosis, we performed a single nucleotide polymorphism-based genome scan in *Sox10^{Dom/+}* F_1 intercross progeny. Our analysis reveals modifier loci on mouse chromosomes 3, 5, 8, 11 and 14 with distinct effects on penetrance and severity of aganglionosis. Three of these loci on chromosomes 3, 8 and 11 do not coincide with previously known aganglionosis susceptibility genes or modifier loci and offer new avenues for elucidating the genetic network that modulates this complex neurocristopathy.

INTRODUCTION

Phenotypes that display non-mendelian inheritance have challenged geneticists to define the genes and mechanisms that contribute to complex disease. Hirschsprung disease (HSCR) is a well-recognized complex disorder characterized by multigenic inheritance, with minimally nine genes (*RET, GDNF, NTN, EDN3, EDNRB, ECE-1, SOX10, ZFHX1B* and *PHOX2B*) contributing to aganglionosis susceptibility in patients (1,2). HSCR is the most common cause of neonatal intestinal obstruction, with a general population incidence of one in 5000 live births. The disorder is clinically identified by the absence of enteric ganglia in a variable portion of the distal gastrointestinal tract. To facilitate genetic analysis, aganglionosis phenotypes in HSCR patients have been subdivided based on the extent of the affected gut segment. Long-segment HSCR (L-HSCR) includes patients with aganglionosis of, and proximal to, the splenic flexure, whereas the remaining cases are grouped as short-segment (S-HSCR) (1,3). Segregation analysis among S-HSCR patients suggests distinct models of segregation with multifactorial or recessive inheritance in effect for S-HSCR, whereas rarer dominant allele models are more consistent with L-HSCR (3). In the cases of isolated HSCR, where aganglionosis is the only

*To whom correspondence should be addressed. Tel: +1 6159362172; Fax: +1 6159362661; Email: michelle.southard-smith@vanderbilt.edu

documented neural crest defect, *RET* mutations are the predominant genetic alteration. Syndromic HSCR, aganglionosis in the context of additional neural crest phenotypes, appears to be the consequence of genetic alteration in genes that are more broadly expressed across neural crest lineages. Regardless of the categorical classification of aganglionosis phenotype (S-HSCR versus L-HSCR; isolated HSCR versus syndromic HSCR), the variable penetrance and expressivity of this disease are attributed to complex genetic interactions between susceptibility loci and undiscovered modifiers in the genetic background that predispose to deficiencies of enteric neural crest (4–6).

Efforts to identify the gene interactions that contribute to phenotypic variation of aganglionic megacolon have focused on the *RET* locus and identified modifiers at 3p21, 9q31, 16q23 and 19q12 (4,7). These loci are hypothesized to result in misregulation of *RET*. Studies in HSCR families and mouse models demonstrate that interactions between *RET* and *EDNRB* also impact disease susceptibility (5,6). Recent molecular and genetic analyses in mice have expanded the gene network to include *Ednrb–Sox10* among the interactions that modulate neural crest cells during enteric nervous system (ENS) ontogeny (8,9). Although *in vitro* studies have suggested that *Sox10* is capable of mediating transcriptional regulation of *Ret* (10), *Sox10* may also impact *Ret* via its interaction with *Ednrb*. Strategies to elucidate the gene interactions that contribute to variation in penetrance and severity of aganglionosis continue to be of great interest because mutations are seldom documented in >30% of total HSCR cases (1).

SOX10 is an essential neural crest transcription factor that is altered in some syndromic HSCR patients (11–13) and in *Dominant megacolon (Sox10^{Dom})* mice (14,15). Patients with *SOX10* alterations typically present with syndromic HSCR defined as aganglionosis associated with other deficits: hypopigmentation, deafness, iridia, nystagmus or ataxia. *Sox10^{Dom}* mice exhibit strain-dependent variation in aganglionosis penetrance and severity analogous to the heterogeneous enteric phenotypes of HSCR patients. This study focuses on the variation in aganglionosis between individual *Sox10^{Dom}* mice and uses this variation to identify modifiers that are influencing the aganglionosis aspect of the phenotype. These studies have been facilitated by the ability to control genetic background in inbred lines of *Sox10^{Dom}* mice that are not possible in patient studies. Previous candidate gene analysis has identified contributions of alleles at *Ednrb* to the variation among individual *Sox10^{Dom}* animals. Yet, only a minor proportion of aganglionosis variance in *Sox10^{Dom}* mice is attributable to the *Ednrb* locus, and the phenotype of *Sox10/Ednrb* double mutants is significantly different on distinct genetic backgrounds (8), implying the existence of additional modifier loci.

The variation in HSCR phenotype and potential number of genes that influence development of the ENS are not surprising when considered in the context of the complex biological processes that neural crest cells endure to populate the gastrointestinal tract. These cells must emigrate from the neural tube, traffic to the foregut, and migrate throughout the intestine, all the while proliferating, and differentiating to give rise to the glia and neurons of the enteric ganglia. Interestingly,
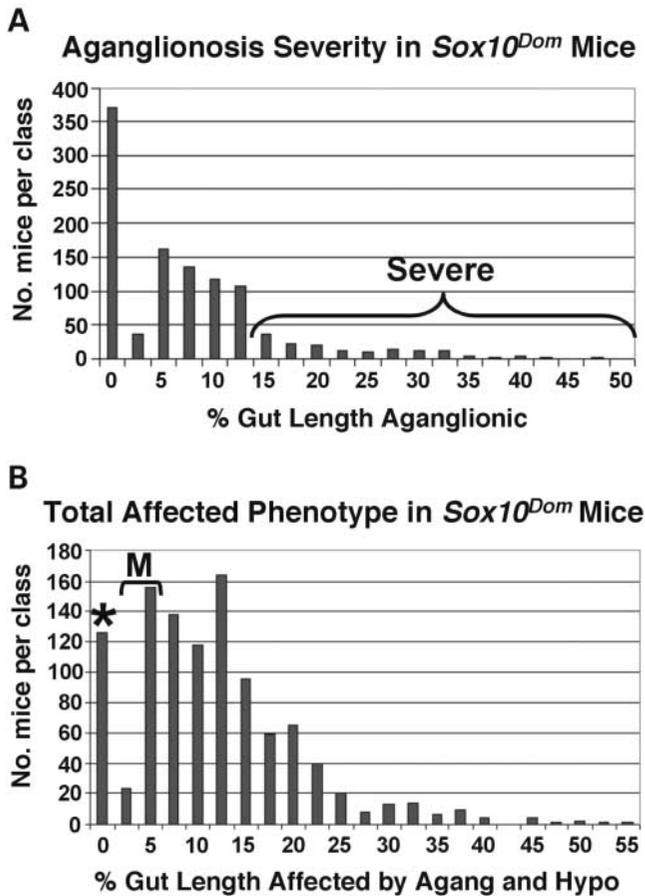
assays of gene expression in enteric neural crest stem cells (NCSC) have established that genes that play a role in aganglionosis susceptibility are highly expressed in these cells and suggest that HSCR is a consequence of NCSC dysfunction (16). *Sox10* is among the genes upregulated in NSCS and maintains both glial and neuronal stem cell potential in the neural crest (17). Consequently, modifiers of *Sox10* are likely to be relevant to neurobiology of enteric stem cells and should further elucidate interacting pathways that are essential for normal development of enteric ganglia.

Candidate gene approaches can be informative, but they are typically based on the biological processes under investigation and are often limited by complete knowledge of all components in a pathway. In contrast, genome-wide linkage studies have the potential to identify essential genes in complex diseases that otherwise would be missed by candidate gene studies (18,19). In this report, we describe a genome-wide survey performed to comprehensively identify *Sox10* modifier loci that affect the penetrance and extent of intestinal aganglionosis. Our analysis reveals modifier loci on mouse chromosomes 3, 5, 8, 11 and 14 that have distinct effects on the penetrance and severity of aganglionosis. Fine-mapping in the modifier interval on chromosome 5, coupled with bioinformatics analysis of genes in the interval, identifies several candidates that are highly relevant based on their expression in enteric neural crest. Our analysis is consistent with the hypothesis that the *Sox10^{Dom}* phenotype is modulated by loci in addition to *Ednrb*. This study contributes significantly to the epistatic network that modulates ENS deficits and will expand our understanding of neural development in the gut.

RESULTS

Evaluation of aganglionosis as a quantitative trait in *Sox10$^{Dom/+}$* F$_2$ mice

To establish the range of phenotypes among *Sox10$^{Dom/+}$* F$_1$ intercross progeny, we evaluated the extent of aganglionosis in postnatal day 7–10 (P7–P10) F$_2$ pups by whole-mount acetylcholinesterase (AChE) histochemistry. AChE staining detects cholinergic neurons in the ENS and is a rapid, high definition method for visualizing ganglia architecture. This technique is advantageous over sectioning because it preserves the three-dimensional organization of the intestinal tissue. All F$_2$ animals ($n = 2210$) were phenotyped and then genotyped for the *Sox10^{Dom}* mutation, with subsequent analyses focusing on *Sox10$^{Dom/+}$* mutants. Genotyping results were consistent with the anticipated 50% transmission ratio, identified 1092 *Sox10$^{Dom/+}$* mice, and confirmed the absence of enteric deficits in all pups that had wild-type genotype. Microscopic examination of *Sox10$^{Dom/+}$* intestines stained by AChE allowed us to score the extent of gut length affected by hypo- and/or aganglionosis in individual animals as a quantitative trait. Consequently, the ready identification of individual mice at the extremes of the phenotype distribution allowed selective genotyping of *Sox10$^{Dom/+}$* animals based either on penetrance (no hypo- or aganglionosis present) (Fig. 1B) or on severity (extent of gut length affected) in the F$_2$ phenotype distribution (Fig. 1A and B).

A

Aganglionosis Severity in *Sox10^Dom* Mice

Severe

No. mice per class / % Gut Length Aganglionic

B

Total Affected Phenotype in *Sox10^Dom* Mice

M

*

No. mice per class / % Gut Length Affected by Agang and Hypo

Figure 1. Evaluation of aganglionosis as a quantitative trait in $Sox10^{Dom/+}$ F_2 mice. Phenotype distribution of aganglionosis (**A**) and total length of the gut affected (**B**) by ENS deficits in $Sox10^{Dom/+}$ F_2 mice. Numbers of mice (*y*-axis) in each phenotype class defined in 2.5% gut length increments are plotted along the *x*-axis. Bracket in (A) identifies the most severely aganglionic 10% of the phenotype distribution ($n = 109$) selected for genotyping. Plot of total affected phenotype in (B) includes both hypoganglionosis and aganglionosis. Animals representing the mildest 10% affected mice (M, $n = 107$) and the non-penetrant animals (asterisk; phenotype of 0% gut length affected, $n = 107$) were selected for genotyping.

Genome-wide linkage analysis identifies modifiers of *Sox10^Dom* aganglionosis penetrance and severity

Selective genotyping of individual animals at the extremes of the phenotype distribution increases the power to detect quantitative trait loci (20,21). We used this approach in our genome survey and determined genotypes of individual F_2 mice with the most severe, mildest or non-penetrant phenotypes ($n = 323$) using single nucleotide polymorphism (SNP) markers. The average initial map resolution of SNP markers spanning all 19 autosomes and the X chromosome was ~18 cM. Because >10% of individual F_2 mice were unaffected, linkage analysis to identify modifier loci was performed using a two-part model (22) that allows for separate effects on penetrance and severity. Significant LOD scores ($P \leq 0.05$) found on chromosomes 3, 5, 8, 11, and 14 indicated the presence of five modifier loci (Fig. 2).

Regions of significant linkage detected in the initial genome scan were investigated further by genotyping all $Sox10^{Dom/+}$ F_2 mice ($n = 1068$) with the marker closest to each significant modifier. In this analysis, the ability to accurately quantify hypoganglionosis, aganglionosis and the total length of gut affected in $Sox10^{Dom/+}$ mice allowed us to assign effects of individual modifiers either on penetrance or severity or on both (Fig. 3). The most significant modifier, on chromosome 5 (chr5) affects the penetrance and severity of both aganglionosis and total affected gut length phenotypes. The other modifier loci on chromosomes 8, 11 and 14 greatly affect penetrance of aganglionosis. Although multipoint LOD plots for these chromosomes demonstrate a notable effect on the severity of the total affected phenotype, this is largely due to individual mice that exhibit hypoganglionosis but no aganglionosis. When the 245 animals with hypoganglionosis but no aganglionosis are excluded (green curves in Fig. 3B), the loci on chromosomes 3, 8, 11 and 14 are seen to have little impact on the severity of the total affected phenotype.

Allele effects of *Sox10^Dom* modifier loci

Modifier loci either can increase susceptibility and severity of phenotype or can act protectively to confer resistance to disease in the face of a predisposing mutation (23). To assess the effects of individual $Sox10^{Dom}$ modifiers (one at a time) on the penetrance and severity of aganglionosis, we evaluated complete genotype information in the total F_2 distribution. B6 alleles at modifier loci on chromosomes 5, 8, 11 and 14 increased both the proportion of individuals affected by aganglionosis and the extent of gut length affected by aganglionosis (Fig. 4). This is consistent with prior reports of more severe phenotype in $Sox10^{Dom/+}$ mutants on the B6 background (8,24,25). In contrast, the chromosome 3 locus exerted an opposite effect with B6 alleles protecting mutants from the presence of aganglionosis and decreasing the severity of aganglionosis. All allele effects observed were approximately additive, with heterozygotes exhibiting phenotypes mid-way between the phenotype ranges of the homozygous animals, consistent with semi-dominant effects of each locus. Complete dominance was not detected for any of the modifier loci.

1.5-LOD support intervals define genomic intervals of *Sox10^Dom* modifier loci

To identify an approximate chromosomal location for each locus, 1.5-LOD support intervals were calculated for each modifier (26) (Fig. 5). Additional genotyping was performed for chromosomes 5, 11 and 14 using 23 additional markers to refine the positions and determine if these peaks were due to more than one modifier on each chromosome. Information for all markers used for genotyping is provided in Supplementary Material Table S1. Although the shape of the LOD curve for chromosome 11 suggested the possibility of multiple modifiers, after controlling for the locus at 42 cM, no further evidence for additional chromosome 11 loci was detected. Analysis of chromosomes 5 and 14 also supported the presence of only a single modifier. The refined mapping narrowed the 1.5-LOD support interval for chr5 to a location at 15–

Multi-point LOD plot from Genome-wide Survey for *Sox10^{Dom}* Modifier Loci
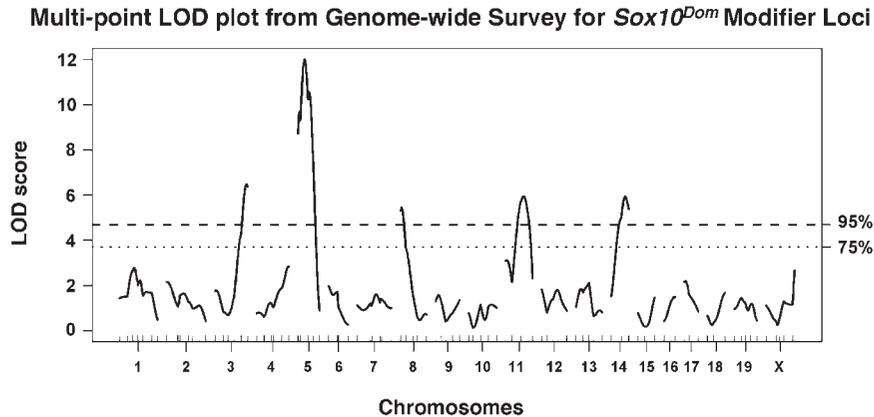
Figure 2. Genome-wide interval mapping of total affected gut length in the phenotypic extremes of the *Sox10^{Dom}* F_2 population. LOD scores from a two-part model indicating the combined effects on penetrance and severity are plotted for all mouse chromosomes revealing five significant modifier loci on chromosomes 3, 5, 8, 11 and 14. Individual chromosomes are listed across the *x*-axis, with tick marks representing the location of SNP markers used in genotyping. Dashed and dotted horizontal lines represent the significant ($P \leq 0.05$) or suggestive ($P \leq 0.25$) thresholds, respectively.

23 cM, whereas the chromosome 11 modifier (chr11) resides in the 1.5-LOD interval at 28–50 cM. The chromosome 14 modifier (chr14) is consistent with the position of *Ednrb* that has been previously reported as a modifier of *Sox10^{Dom}* (8). The chr14 locus was initially detected by our genome-wide linkage analysis using SNP markers on chromosome 14, which were evenly distributed along the chromosome and independent of the markers previously used in candidate gene studies (8). Subsequently, we incorporated genotype data from additional markers flanking the *Ednrb* locus into the analysis to obtain the narrowed linkage interval centered at 54 cM.

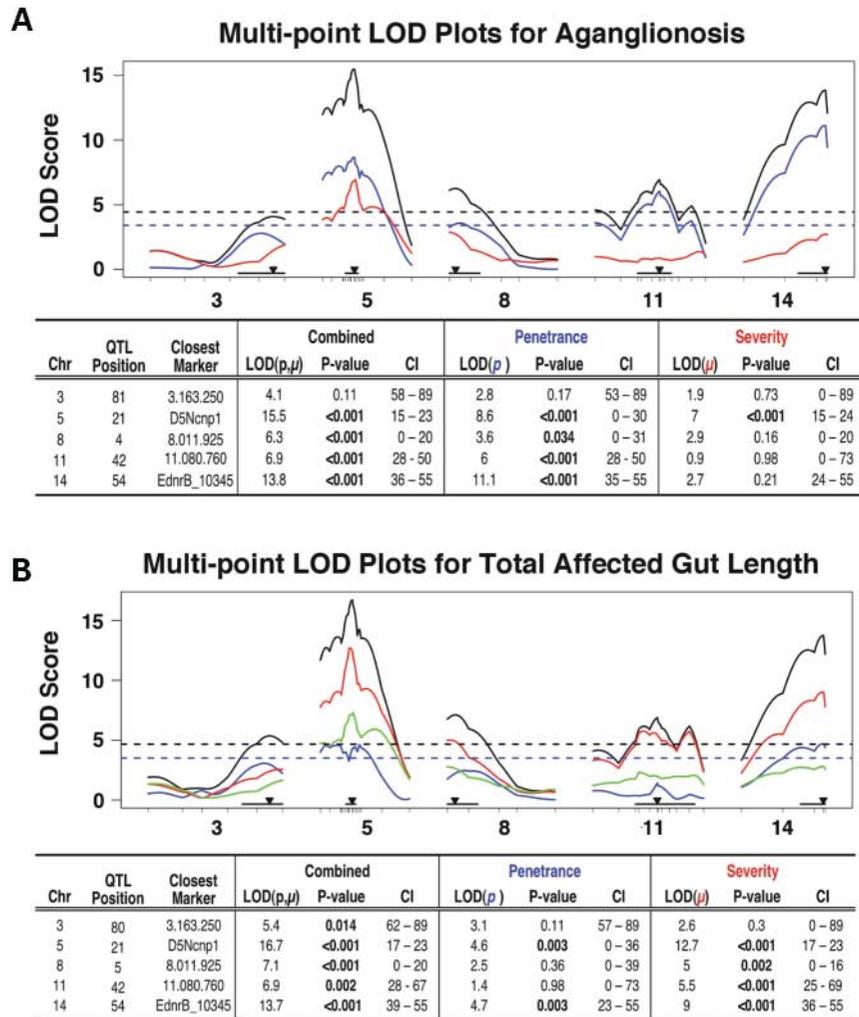### Identification of candidate genes in chromosome 5 modifier interval

Bioinformatics approaches combining genome annotation with literature searches have been used successfully to identify biologically relevant genes within modifier intervals (27). We used the positions of the closest markers flanking the 1.5-LOD interval on chr5 to define the boundaries of this interval on the mouse genome assembly and search for genes that might be involved in development of enteric neural crest based on their expression profiles in the literature and public databases. A total of 59 genes within this interval were identified by Ensembl Martview (28). This listing of candidates was narrowed to include only those genes with reported expression in the embryo and in the gastrointestinal tract based on information in the PubMed and in the Gene Expression Database (29) (Table 1). Within this focused list, several highly relevant candidates were identified based on their documented expression in enteric neural crest cells in the developing gut. These include *Uchl1* (PGP9.5), *Atp8a1* and *Phox2b*. *Uchl1*, a ubiquitin ligase, is expressed early in the development of enteric neurons and maintained in mature neurons. Expression of *Atp8a1*, an aminophospholipid translocase, has been reported in embryonic enteric precursors but the developmental timing or cell-type specificity has not been determined

(30). *Phox2b* is expressed in early enteric neural progenitors, maintained in differentiating neurons (31–33) and ablation of the gene leads to complete loss of enteric neurons in mice (34). It is notable that *PHOX2B* mutations have been reported in Haddad syndrome patients that exhibit features of central congenital hypoventilation defects syndrome in association with aganglionosis (2,35). Expansions of the second polyalanine tract in *PHOX2B* have been associated with severity of the neural crest defects in this syndrome (36) and specific haplotypes at *PHOX2B* are over-represented in HSCR patients in case–control studies (37). *Phox2b* is a logical and exciting candidate modifier for future study.

DISCUSSION

Variation in expressivity and penetrance of HSCR is the consequence of multiple gene interactions that modulate the ability of enteric neural crest cells to populate the developing gut. *Sox10* is a key transcriptional regulator, which is integral to the processes of ENS development. To identify the genome locations of new genes that impact ENS development and thus aganglionosis, we have undertaken a genome-wide linkage analysis in *Sox10^{Dom/+}* mice. Our study was designed to detect genetic modifiers, regions of the genome that do not exhibit an obvious phenotype, but in the context of the *Sox10^{Dom}* mutation, exert an effect on the penetrance and severity of aganglionosis. Using this comprehensive approach, we have successfully identified five modifier loci of *Sox10^{Dom}* on mouse chromosomes 3, 5, 8, 11 and 14.

We have demonstrated the value of defining aganglionosis as a quantitative trait in mouse models to map modifiers of aganglionic megacolon. Our approach allows us to estimate the genetic contribution to this phenotype and establishes that there is a significant genetic contribution to *Sox10^{Dom}* hypoganglionosis ($h^2 = 0.52$), aganglionosis ($h^2 = 0.60$) and total affected phenotypes ($h^2 = 0.66$). This is consistent with previous reports of genetic background effects on *Sox10* phenotypes (8,12,24,38 and 39). Importantly, phenotype

A

Multi-point LOD Plots for Aganglionosis

Chr	QTL Position	Closest Marker	Combined			Penetrance			Severity		
			LOD(p,μ)	P-value	CI	LOD(p)	P-value	CI	LOD(μ)	P-value	CI
3	81	3.163.250	4.1	0.11	58 – 89	2.8	0.17	53 – 89	1.9	0.73	0 – 89
5	21	D5Ncnp1	15.5	<0.001	15 – 23	8.6	<0.001	0 – 30	7	<0.001	15 – 24
8	4	8.011.925	6.3	<0.001	0 – 20	3.6	0.034	0 – 31	2.9	0.16	0 – 20
11	42	11.080.760	6.9	<0.001	28 – 50	6	<0.001	28 – 50	0.9	0.98	0 – 73
14	54	EdnrB_10345	13.8	<0.001	36 – 55	11.1	<0.001	35 – 55	2.7	0.21	24 – 55

B

Multi-point LOD Plots for Total Affected Gut Length

Chr	QTL Position	Closest Marker	Combined			Penetrance			Severity		
			LOD(p,μ)	P-value	CI	LOD(p)	P-value	CI	LOD(μ)	P-value	CI
3	80	3.163.250	5.4	0.014	62 – 89	3.1	0.11	57 – 89	2.6	0.3	0 – 89
5	21	D5Ncnp1	16.7	<0.001	17 – 23	4.6	0.003	0 – 36	12.7	<0.001	17 – 23
8	5	8.011.925	7.1	<0.001	0 – 20	2.5	0.36	0 – 39	5	0.002	0 – 16
11	42	11.080.760	6.9	0.002	28 – 67	1.4	0.98	0 – 73	5.5	<0.001	25 – 69
14	54	EdnrB_10345	13.7	<0.001	39 – 55	4.7	0.003	23 – 55	9	<0.001	36 – 55

Figure 3. Modifier loci defined by genotyping the total $Sox10^{Dom/+}$ F$_2$ population exhibit distinct effects on penetrance and severity. Multipoint LOD plots for the five modifier loci on chromosomes 3, 5, 8, 11 and 14 are shown. For each modifier locus, LOD scores indicating the effect on penetrance (the chance of being affected, blue curves), severity (the average amount affected given that there is an effect, red curves) or both (black curves) was evaluated for two phenotypic subsets: aganglionosis (**A**) and total length of affected gut (**B**). Tick marks on the *x*-axis representing the location of markers used to genotype each chromosome. The horizontal dashed lines indicating the 95% LOD thresholds for LOD (p, μ) in black and the 95% LOD thresholds for LOD (p) and LOD (μ) in blue. Inset tables list the position (in centiMorgans) of each modifier locus, the closest marker used for genotyping in the total F$_2$ distribution, and LOD scores, *P*-values and 95% confidence intervals (CI). LOD curves for severity in (A) (in red) derive from considering animals with aganglionosis more than zero ($n = 700$). LOD curves for severity in (B) (in red) derive from considering animals with total affected gut length more than zero ($n = 945$). In (B) several modifiers appear to affect the severity of total affected gut length, but this is largely attributable to individuals with hypoganglionosis greater than zero and with aganglionosis equal to zero. When the severity of total affected phenotype is considered for only those animals with aganglionosis greater than zero (green curves, B), it becomes clear that the apparent contribution of loci on chromosomes 3, 8, 11 and 14 to severity of total affected phenotype is attributable to animals with hypoganglionosis but not aganglionosis.

evaluation in mouse mutants like $Sox10^{Dom}$ is not limited by practical challenges associated with obtaining biopsy materials in human HSCR patients. Our characterization of $Sox10^{Dom}$ phenotype illustrates that enteric deficits are present as a continuum ranging from extremely severe aganglionosis to unaffected animals. In human HSCR, *SOX10* mutations have been more frequently documented in syndromic HSCR cases (11,13), but reports of non-penetrant individuals with *SOX10* alterations have been documented (12). Previous genetic studies of HSCR have attempted to simplify phenotypes by classifying patients into L-HSCR and S-HSCR categories based on the extent of gastrointestinal tract affected (3). Our

characterization of $Sox10^{Dom}$ phenotype suggests that categorical classification of patients may be an over-simplification that could dilute the power to detect all modifier loci involved in a complex phenotype like aganglionosis. Although comparable studies have not been performed in *Ret* mouse models to investigate the effects of genetic background and range of phenotype, studies in HSCR patients indicate that aganglionosis also varies widely in *RET* patients (1,7,40).
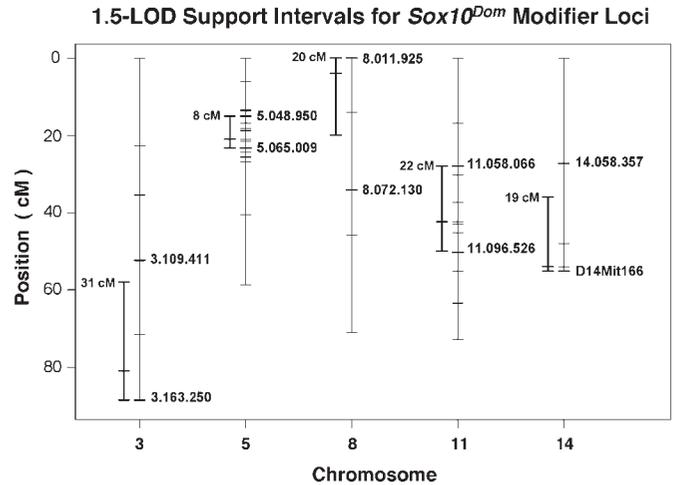
Although chr14 position and allele effects are consistent with prior reports of *Ednrb* affecting aganglionosis in *Sox10* mutants, three of the five modifier loci we identify map to novel regions on chromosomes 3, 8, and 11 that have not
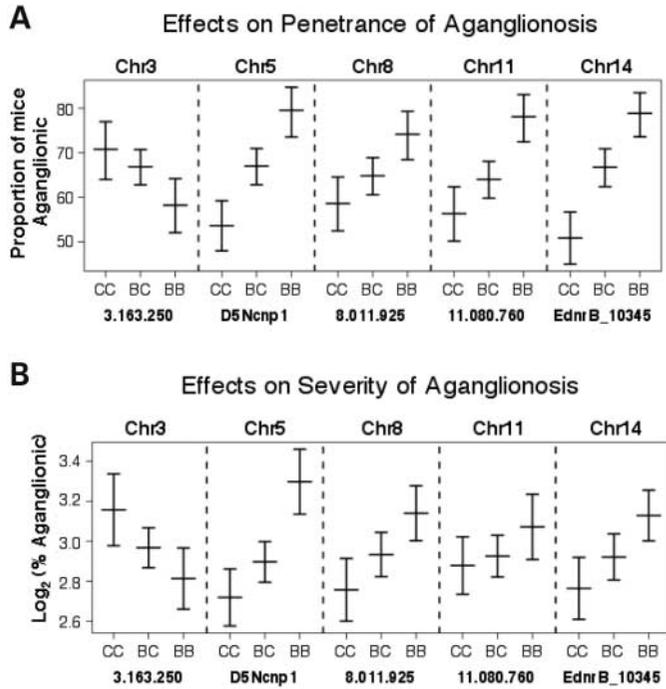
Figure 4. Effect of alleles at $Sox10^{Dom}$ modifier loci on the penetrance and severity of aganglionosis. Genotypes from the total F_2 population obtained from the marker closest to each significant modifier were used to assess the effects of individual loci (one at a time) on penetrance (A) and severity (B) of phenotype. In (A) the estimate (midline) and 95% confidence interval (flanking brackets) of the probability that an individual with a certain genotype at the individual modifier loci will exhibit aganglionosis is plotted for each genotype class to illustrate the relationship between the number of B6 or C3Fe alleles at each modifier locus and the presence of aganglionosis. (B) The mean of the log_2 transformed percentage aganglionosis is plotted for each genotype class to show the relation of the number of B6 or C3Fe alleles and the extent of aganglionosis. Markers used to generate genotype information are listed beneath the plot for each locus. Genotype groups are defined as B6/B6 (BB), B6/C3Fe (BC) and C3Fe/C3Fe (CC).

Figure 5. Refined intervals of modifier loci. Plots of 1.5-LOD support intervals show the position and size of significant intervals for the modifier loci on chromosomes 3, 5, 8, 11 and 14. Chromosomes containing significant modifiers are plotted against map position. Vertical lines represent the entire length of each chromosome with tick marks representing the position of the markers used to genotype the chromosome. The vertical brackets in bold to the left of each chromosome indicate the 1.5-LOD support interval for aganglionosis and the tick mark in the middle of the bracket shows the estimated position of the modifier. The total span (in centiMorgans) of the support interval is reported at the top of each bracket. The name of the markers flanking the 1.5-LOD support interval are shown.

been previously associated with HSCR. These novel modifier intervals do not coincide with syntenic regions of known aganglionosis susceptibility loci (*RET, GDNF, NTN, EDN3, EDNRB, ECE-1, SOX10* and *ZFHX1B*) or previously mapped modifiers in HSCR patients (3p21, 19q12, 9q31 or 16q23) (4,5,7). Moreover, we determined that essential genes for neural crest development including *Grb10, Pax3, Phox2a, dHand, Hox11L1, Krox20, Mash1, Pou3f1, Kit, Ednrbm1, Hoxa4, Dlx2* and *Ikbkap* do not map to these regions. *Sox8* has been recently reported as a modifier of aganglionosis in mice haploinsufficient for *Sox10* based on the increased extent of aganglionosis in double mutant $Sox10^{LacZ/+}$, $Sox8^{LacZ/LacZ}$ mice (41). However, none of the modifier loci identified in our study map to the same location as *Sox8*, and no previous evidence suggests that naturally occurring variants at *SOX8* influence HSCR.

It is possible that the chr5 modifier locus we identified is equivalent to *Phox2b* and if substantiated would offer significant support for the mechanistic view of HSCR as a stem cell disorder. *Sox10–Phox2b* interaction would be consistent with prior descriptions of HSCR as a stem cell defect (16) because

the most likely temporal window for interaction between these two genes would occur in the NCSC just before or during early migration into the gut. In support of this hypothesis, Kim *et al.* (17) have reported co-expression of *Phox2b* in Sox10+ neural crest cells and loss of *Phox2b* expression in homozygous $Sox10^{Dom/Dom}$ embryos.

HSCR inheritance is complicated by epistasis, gender and parent-of-origin effects (1,7). The modifier loci identified in this study are, by definition, in epistasis with *Sox10*. However, when we tested pairwise interactions between the modifiers identified in our analysis, we saw no evidence for epistasis between these loci (data not shown). Gender effects in isolated human HSCR where *RET* alterations are the predominating alteration show a marked 4:1 predominance of males/females (3). Gender effects on penetrance of aganglionosis have also been reported for patients with alterations in *ENDRB* (42). There is not a greater incidence or severity of aganglionosis in $Sox10^{Dom/+}$ males than in females. We previously reported a small gender specific effect for the direction of dominance at the *Ednrb* locus on the severity of aganglionosis in $Sox10^{Dom/+}$ mutants (8). Our current findings are consistent with that result. In both cases, the analysis derived from comparison of C57BL/6J with C3 substrains, C3FeLe.B6-a and C3HeB/FeJ, respectively, and may reflect the common origin of these substrains. In our genome survey, we anticipated the potential to identify significant gender or parent-of-origin effects and established our crosses to facilitate detection; however, we observed little evidence for notable gender or parent-of-origin effects when we tested for these effects at the newly identified modifier loci. This is consistent with prior observations that notable gender effects have only been documented for *RET* and

**Table 1.** Candidate genes identified within the chromosome 5 modifier interval

Gene name	Description	Expression
Pgm1	Phosphoglucomutase	Widely expressed: including postnatal small intestine and colon
Klf3	Kruppel-like factor 3 (CACCC-box binding transcriptional repressor)	Widely expressed: including postnatal small and large intestine
Tlr1	Toll-like receptor 1 precursor	Widely expressed: including immune cells and adult colon
Recc1	Activator 1 140 kDa subunit (Replication factor C large subunit)	Widely expressed: including postnatal and adult colon, germ cells
Ugdh	UDP-glucose 6-dehydrogenase (EC 1.1.1.22; UDP-GlcDH)	Postnatal and adult colon, teeth, neuroblasts, skin, retina
Hip2	Ubiquitin-conjugating enzyme E2-25 kDa (EC 6.3.2.19; Huntingtin interacting protein 2)	Widely expressed: including postnatal colon
Uchl1	Ubiquitin C-terminal hydrolase isozyme L1 (EC 3.4.19.12; Neuron cytoplasmic protein PGP 9.5)	Embryonic enteric precursors and adult gut; peripheral nervous system, brain, embryonic eye, ear and heart, postnatal ovary, oocytes and pituitary, salivary gland
Phox2b	Paired mesoderm homeobox protein 2B, transcription factor	Embryonic enteric precursors, adult gut, brain
Slc30a9	Solute carrier family 30 member 9 (zinc transporter)	Widely expressed: including adult colon, brain, teeth, skin, lymphoblasts
Atp8a1	Potential phospholipid-transporting ATPase IA (EC 3.6.3.1; Chromaffin granule ATPase II)	Embryonic enteric precursors, brain, skin, thymus, teeth, vagina

Statistical analysis identified two SNP markers, 5.048.950 and 5.065.009, which flanked the 1.5-LOD support interval for the chr5 locus. The immediate sequence surrounding these markers (49) was used to identify by BLASTN alignment (version 2.2.10) the base pair positions of these markers on the current mouse genome assembly. On Build 33c (accessed 12/8/04) marker 5.048.950 was positioned at 53 218 105 bp, and 5.065.009 was identified at 69 383 575 bp. These positions were used in Ensembl 'MartView' (http://www.ensembl.org/Multi/martview/w3Q7eoEaQN.mart) to identify all genes within the interval flanked by these markers. Information on the expression of each gene within the interval was collected from the primary literature (PubMed; http://www.ncbi.nlm.nih.gov/entrez/query.fcgi?db=PubMed) or MGI (http://www.informatics.jax.org/). The listing of candidates was narrowed to include only those genes with reported expression in the embryo and in the gut. Highly relevant candidate genes known to be expressed in enteric precursors in embryonic gut are shown in bold.

EDNRB in human HSCR cases (1,42). It is possible that genome regions capable of exerting gender and parent-of-origin effects on $Sox10^{Dom}$ phenotypes are equivalent between the B6 and the C3Fe strains that we have investigated. Future studies of $Sox10^{Dom/+}$ mutants in additional strain backgrounds will determine whether *Sox10* phenotypes are subject to the same gender and parent-of-origin effects observed in human HSCR or if these characteristics are unique to the *RET* and *EDNRB* loci and their modifiers.

We have summarized the gene interactions detected in this study and tried to define them in the context of what is known to date about epistatic effects in HSCR (Fig. 6). Others have established epistasis between *Ret* and *Ednrb* (5,6), while prior studies from our group identified effects of *Sox10–Ednrb* on aganglionosis phenotypes in $Sox10^{Dom/+}$ mutants. We did not detect any genetic interaction between *Ret* and *Sox10* in our analysis despite prior *in vitro* studies suggesting *Sox10* directly regulates *Ret* transcription (10). However, we strongly suspect that the B6 and C3Fe strains carry equivalent haplotypes through the *Ret* interval because screens to identify polymorphic markers in the immediate proximity of the *Ret* locus were not successful (V.A. Cantrell and E.M. Southard-Smith, unpublished data). *Ret* and *Sox10* may exhibit epistasis in other strains that are divergent through the *Ret* interval. Given that *Sox10* directly modulates *Ednrb* transcription (9), it is also possible that *Sox10* may influence *Ret* activity via its interaction with *Ednrb*.

Our study does not exclude the potential for other HSCR modifiers and interactions that might be detected in additional strains, but instead emphasizes the value of investigating heterogeneous disorders like HSCR in mouse models where genetic background and input alleles can be controlled to provide additional power for genetic analysis.
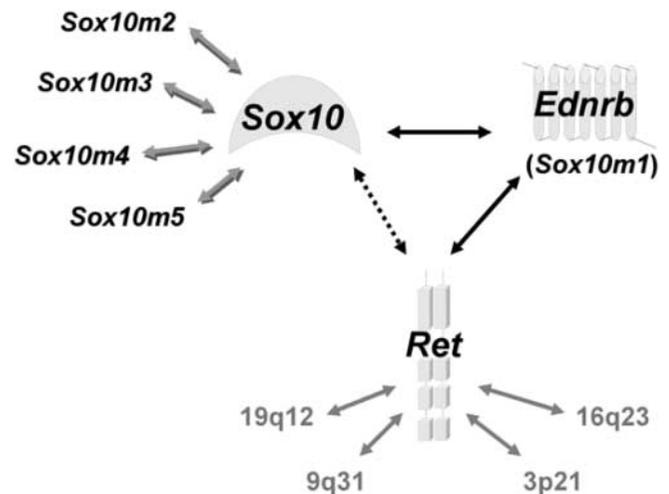
Figure 6. Summary of gene interactions that contribute to heterogeneity of aganglionosis in HSCR. Heavy black arrows represent genetic interactions validated by analysis of double mutants *in vivo*. Lighter gray arrows indicate *RET*-dependent modifiers detected in human genetic studies. Effects of the 16q23 locus, although apparently confined to inbred Mennonite populations (5) may further inform the process of ENS development. Dashed arrow emphasizes potential for gene interaction between *Sox10* and *Ret* based on *in vitro* studies. Modifiers of *Sox10* identified in this study (*Sox10m1-5*) are shown in black text accompanied by gray shadowed arrows.

MATERIALS AND METHODS

Mice

All animal protocols were approved by the Institutional Animal Care and Use Committee at Vanderbilt University.

Table 2. Source crosses for generation of F_1 intercross progeny

Source cross	Number of breeding pairs[a]	Number of $Sox10^{Dom/+}$ Progeny
Female (C3Fe $\times$ B6) $F_1\times$male (C3Fe$\times$B6.Dom) F_1	8	260
Female (B6$\times$C3Fe) $F_1\times$male (B6.Dom$\times$C3Fe) F_1	5	210
Female (B6.Dom$\times$C3Fe) $F_1\times$male (B6$\times$C3Fe) F_1	7	283
Female (C3Fe$\times$B6.Dom) $F_1\times$male (C3Fe$\times$B6) F_1	10	315
Pups found dead before P7, no gut collected	NA	24
Total	30	1092

[a]Number of breeding pairs is defined as the number of $Sox10^{Dom/+}$ parental mice used in each source cross. NA, not applicable.

Lines of $Sox10^{Dom/+}$ mice congenic on the C57BL/6J background (B6$_{N14}$.$Sox10^{Dom/+}$) were crossed with C3HeB/FeJ (C3Fe) mice to generate B6$_{N15}$C3Fe.$Sox10^{Dom/+}$ (F_1) progeny. Intercrosses were performed by crossing male B6$_{N15}$-C3Fe.$Sox10^{Dom/+}$ (F_1) mice to wild-type B6C3Fe or C3FeB6 females as well as reciprocal intercrosses between female B6$_{N15}$C3Fe.$Sox10^{Dom/+}$ (F_1) mice and wild-type B6C3Fe or C3FeB6 males in order to explore the effects of imprinting (Table 2). From these crosses, 2210 F_2 mice were generated. Of the total cohort, tissues were collected from 2184 animals for evaluation of ENS deficits. Gut tissues from P7–P10 pups were collected and processed for acetycholinesterase whole-mount staining (AChE) using routine protocols (8) to visualize enteric ganglia. The extent of gut regions affected by either hypoganglionosis or aganglionosis was determined by microscopic examination. The entire length of the gut, as well as any hypo- or aganglionic regions, was measured. Lengths of the hypo- or aganglionic segment were divided by the total length of the gut to yield percentage of hypoganglionosis or percentage of aganglionosis. Total affected percentage was defined as the sum of percentage of hypoganglionosis and percentage of aganglionosis. Subsequent to AChE staining and quantitation of ENS deficits, animals were genotyped for gender and the presence of the $Sox10^{Dom}$ allele as described previously (15,43). Selective genotyping of individual animals at the extremes of the phenotype distribution was performed as described by Silver (44). Briefly, from the total distribution of 1068 $Sox10^{Dom/+}$ animals, 109 F_2 mice that represented the most severely aganglionic 10% from the tail of the phenotype distribution were selected and 107 F_2 mice that represented the 10% most mildly affected were selected from the opposite tail of the distribution. To evaluate modifiers of penetrance, 107 (out of 126 total) non-penetrant F_2 animals (phenotype of 0% gut length affected) were selected for genotyping.

Marker selection and detection

SNP markers selected on the basis of polymorphism between C57BL/6J and C3H/HeJ strains of mice were identified either from publicly available databases at the Whitehead Institute (www.genome.wi.mit.edu/SNP/mouse) and the Roche database (http://mouseSNP.roche.com) or from SNP screens performed at Novartis Research Foundation. A total of 98 SNP markers spanning all 19 autosomes and the X chromosome were chosen for the initial genome scan with an average inter-marker distance of $\sim$18 cM. Twelve additional markers were applied in genotyping the tails of F_2 phenotype distribution to refine the modifier interval on chromosome 5. Eight additional markers on chromosome 11 were likewise selected for genotyping to refine the broad interval and allow for further analysis of epistatic effects. Simple sequence length polymorphism markers neighboring *Ednrb* and *Sox10* were also genotyped and included as components of the genome scan. In total, 121 markers (Supplementary Material, Table S1) were used for genotyping.

SNP genotypes were generated by single nucleotide primer extension with detection by fluorescence polarization (FP) (45). Reaction processing entailed three steps: a 4.2 μl PCR reaction, addition of 4 μl of an ExoI and CIP reagent mix to degrade unincorporated primer and dephosphorylate dNTPs and a final addition of 4 μl of an Acyclopol and Acycloterminator reagent mix for the primer extension reaction (AcycloPrime^{TM}-FP SNP Detection System, Perkin–Elmer, Boston, MA, USA). Each 4.2 μl of PCR mixture included 0.1 unit AmpliTaq Gold DNA polymerase, 1$\times$ Buffer II (Applied Biosystems, Foster City, CA, USA), 2.5 mM MgCl$_2$, 0.25 mM dNTPs, 335 nM of each primer, and 2 ng DNA. Integrated automation was employed for genotyping in 384-well format (Tecan Genesis Workstation 200, Tecan GenMate, Velocity11 VSpin and MJ Tetrads). Incorporation of R110- and TAMRA-labeled Acycloterminators was detected by FP on a Molecular Devices/LJL Analyst HT. Samples were genotyped in duplicate and in a few cases in triplicate to obtain the least number of uncalled genotypes possible for each marker in the total 326 samples assayed in the initial genome scan and for the closest marker to each modifier locus in the total F2 progeny of 1068 samples.

Statistical analysis

The heritability (h^2) of ENS deficits in $Sox10^{Dom}$ mice was established by calculating the proportion of genetic variance to total variance $[(V_{f2} - V_{f1})/(V_{f2})]$, where V_{f2} is the phenotypic variance observed within the $Sox10^{Dom}$ F_2 intercross progeny ($n = 1068$) and V_{f1} is the phenotypic variance within the $Sox10^{Dom}$ F_1 parents ($n = 39$) used to perform the intercross. The heritability factor was calculated for three phenotypes: aganglionosis ($h^2 = 0.60$), hypoganglionosis ($h^2 = 0.52$), and total affected ($h^2 = 0.66$). The significant genetic contribution to these phenotypes is consistent with previous reports of genetic background effects in congenic lines (8,24).

Table 3. Phenotype classes of $Sox10^{Dom}$ F$_2$ mice

$Sox10^{Dom/+}$ Phenotype	Number of $Six10^{dom/+}$ F$_2$ mice
'Unaffected', neither hypo- nor aganglionosis present	123
'Hypo only', no aganglionosis present	245
'Agang only', no hypoganglionosis present	3
'Both', hypo- and aganglionosis present	697

In the 'agang only' phenotype class, all three individuals had no hypo, but a large extent of aganglionosis; therefore three classifications were used in the analysis: unaffected ($n = 123$)/hypo only ($n = 245$)/aganglionosis ($n = 700$).

The total distribution of $Sox10^{Dom}$ F2 animals comprised the following subsets in Table 3.

Statistical analyses to identify modifiers of $Sox10^{Dom}$ were performed via a two-part model (22), an extension of standard interval mapping appropriate for the case in which many individuals exhibit a non-penetrant phenotype of zero. We considered a single-modifier model and assumed that an individual with modifier genotype g has probability p_g of having a non-zero phenotype; and that, given its phenotype is greater than zero, it follows, approximately, a normal distribution with mean μ_g and standard deviation σ. We calculated three sets of LOD scores, to indicate the evidence for the presence of modifiers: LOD(p) concerns the test of the hypothesis that $p_g = p$ for all g, the penetrance; LOD(μ) concerns the test of the hypothesis that $\mu_g = \mu$ for all g, the severity. LOD(p, μ) combines the two. A log base 2 transformation was performed on all three phenotypes to attenuate the great skew in their distributions. Statistical analyses were performed with R/qtl version $0.99-9$ (46).

Statistical significance was assessed via permutation tests (47), with 1000 permutation replicates. Interval estimates of modifier location were calculated via 1.5-LOD support intervals, which correspond to $\sim$95% confidence intervals (48).

Gender and parent-of-origin effects were assessed by splitting the data according to such covariates and by the inclusion of sex and/or parent-of-origin as additive covariates in the modifier analyses.

The possibility of epistasis (interactions between modifiers) was assessed by testing for pairwise interactions between the loci identified in the single-modifier analyses. The possibility of multiple modifiers on chromosome 11, suggested by the multiple peaks in the LOD curve, was assessed by a two-dimensional, two-QTL scan of chromosome 11 only, and with the loci on chromosomes 3, 5, 8 and 14, included as additive covariates.

Nomenclature

The chromosome intervals that exert the specific effects on $Sox10^{Dom}$ penetrance and aganglionosis described in this manuscript have been approved by the Mouse Genome Informatics Nomenclature committee for designation as modifier loci: $Sox10m1$ (chr14), $Sox10m2$ (chr3), $Sox10m3$ (chr5), $Sox10m4$ (chr8) and $Sox10m5$ (chr11).

SUPPLEMENTARY MATERIAL

Supplementary Material is available at HMG Online.

REFERENCES

1. Chakravarti, A., McCallion, A.S. and Lyonnet, S. (2004) Hirschsprung Disease. In *The Metabolic and Molecular Bases of Inherited Disease.* The McGraw-Hill Companies New York, NY, Chapter 251, Vol. 2004, 1–47.
2. Amiel, J., Laudier, B., Attie-Bitach, T., Trang, H., de Pontual, L., Gener, B., Trochet, D., Etchevers, H., Ray, P., Simonneau, M. *et al.* (2003) Polyalanine expansion and frameshift mutations of the paired-like homeobox gene PHOX2B in congenital central hypoventilation syndrome. *Nat. Genet.*, **33**, 459–461.
3. Badner, J.A., Sieber, W.K., Garver, K.L. and Chakravarti, A. (1990) A genetic study of Hirschsprung disease. *Am. J. Hum. Genet.*, **46**, 568–580.
4. Bolk, S., Pelet, A., Hofstra, R.M., Angrist, M., Salomon, R., Croaker, D., Buys, C.H., Lyonnet, S. and Chakravarti, A. (2000) A human model for multigenic inheritance: phenotypic expression in Hirschsprung disease requires both the RET gene and a new 9q31 locus. *Proc. Natl Acad. Sci. USA*, **97**, 268–273.
5. Carrasquillo, M.M., McCallion, A.S., Puffenberger, E.G., Kashuk, C.S., Nouri, N. and Chakravarti, A. (2002) Genome-wide association study and mouse model identify interaction between RET and EDNRB pathways in Hirschsprung disease. *Nat. Genet.*, **32**, 237–244.
6. McCallion, A.S., Stames, E., Conlon, R.A. and Chakravarti, A. (2003) Phenotype variation in two-locus mouse models of Hirschsprung disease: tissue-specific interaction between Ret and Ednrb. *Proc. Natl Acad. Sci. USA*, **100**, 1826–1831.
7. Gabriel, S.B., Salomon, R., Pelet, A., Angrist, M., Amiel, J., Fornage, M., Attie-Bitach, T., Olson, J.M., Hofstra, R., Buys, C. *et al.* (2002) Segregation at three loci explains familial and population risk in Hirschsprung disease. *Nat. Genet.*, **31**, 89–93.
8. Cantrell, V.A., Owens, S.E., Chandler, R.L., Airey, D.C., Bradley, K.M., Smith, J.R. and Southard-Smith, E.M. (2004) Interactions between Sox10 and EdnrB modulate penetrance and severity of aganglionosis in the Sox10Dom mouse model of Hirschsprung disease. *Hum. Mol. Genet.*, **13**, 2289–2301.
9. Zhu, L., Lee, H.O., Jordan, C.S., Cantrell, V.A., Southard-Smith, E.M. and Shin, M.K. (2004) Spatiotemporal regulation of endothelin receptor-B by SOX10 in neural crest-derived enteric neuron precursors. *Nat. Genet.*, **36**, 732–737.
10. Lang, D. and Epstein, J.A. (2003) Sox10 and Pax3 physically interact to mediate activation of a conserved c-RET enhancer. *Hum. Mol. Genet.*, **12**, 937–945.
11. Pingault, V., Bondurand, N., Kuhlbrodt, K., Goerich, D.E., Prehu, M.O., Puliti, A., Herbarth, B., Hermans-Borgmeyer, I., Legius, E., Matthijs, G. *et al.* (1998) SOX10 mutations in patients with Waardenburg–Hirschsprung disease. *Nat. Genet.*, **18**, 171–173.
12. Southard-Smith, E.M., Angrist, M., Ellison, J.S., Agarwala, R., Baxevanis, A.D., Chakravarti, A. and Pavan, W.J. (1999) The Sox10(Dom) mouse: modeling the genetic variation of Waardenburg–hah (WS4) syndrome. *Genome Res.*, **9**, 215–225.
13. Inoue, K., Khajavi, M., Ohyama, T., Hirabayashi, S., Wilson, J., Reggin, J.D., Mancias, P., Butler, I.J., Wilkinson, M.F., Wegner, M. *et al.* (2004) Molecular mechanism for distinct neurological phenotypes conveyed by allelic truncating mutations. *Nat. Genet.*, **36**, 361–369.

14. Herbarth, B., Pingault, V., Bondurand, N., Kuhlbrodt, K., Hermans-Borgmeyer, I., Puliti, A., Lemort, N., Goossens, M. and Wegner, M. (1998) Mutation of the Sry-related *Sox10* gene in Dominant megacolon, a mouse model for human Hirschsprung disease. *Proc. Natl Acad. Sci. USA*, **95**, 5161–5165.

15. Southard-Smith, E.M., Kos, L. and Pavan, W.J. (1998) Sox10 mutation disrupts neural crest development in Dom Hirschsprung mouse model. *Nat. Genet.*, **18**, 60–64.

16. Iwashita, T., Kruger, G.M., Pardal, R., Kiel, M.J. and Morrison, S.J. (2003) Hirschsprung disease is linked to defects in neural crest stem cell function. *Science*, **301**, 972–976.

17. Kim, J., Lo, L., Dormand, E. and Anderson, D.J. (2003) SOX10 maintains multipotency and inhibits neuronal differentiation of neural crest stem cells. *Neuron*, **38**, 17–31.

18. Lander, E.S. and Schork, N.J. (1994) Genetic dissection of complex traits. *Science*, **265**, 2037–2048.

19. Mogil, J.S., Wilson, S.G., Chesler, E.J., Rankin, A.L., Nemmani, K.V., Lariviere, W.R., Groce, M.K., Wallace, M.R., Kaplan, L., Staud, R. *et al.* (2003) The melanocortin-1 receptor gene mediates female-specific mechanisms of analgesia in mice and humans. *Proc. Natl Acad. Sci. USA*, **100**, 4867–4872.

20. Darvasi, A. and Soller, M. (1992) Selective genotyping for determination of linkage between a marker locus and a quantitative trait locus. *Theor. Appl. Genet.*, **83**, 353–359.

21. van Gestel, S., Houwing-Duistermaat, J.J., Adolfsson, R., van Duijn, C.M. and van Broeckhoven, C. (2000) Power of selective genotyping in genetic association analyses of quantitative traits. *Behav. Genet.*, **30**, 141–146.

22. Broman, K.W. (2003) Mapping quantitative trait loci in the case of a spike in the phenotype distribution. *Genetics*, **163**, 1169–1175.

23. Nadeau, J.H. (2003) Modifier genes and protective alleles in humans and mice. *Curr. Opin. Genet. Dev.*, **13**, 290–295.

24. Lane, P.W. and Liu, H.M. (1984) Association of megacolon with a new dominant spotting gene (Dom) in the mouse. *J. Hered.*, **75**, 435–439.

25. Kapur, R.P., Livingston, R., Doggett, B., Sweetser, D.A., Siebert, J.R. and Palmiter, R.D. (1996) Abnormal microenvironmental signals underlie intestinal aganglionosis in Dominant megacolon mutant mice. *Dev. Biol.*, **174**, 360–369.

26. Broman, K.W. (2001) Review of statistical methods for QTL mapping in experimental crosses. *Lab Animal*, **30**, 44–52.

27. Cozma, D., Lukes, L., Rouse, J., Qiu, T.H., Liu, E.T. and Hunter, K.W. (2002) A bioinformatics-based strategy identifies c-Myc and Cdc25A as candidates for the Apmt mammary tumor latency modifiers. *Genome Res.*, **12**, 969–975.

28. Kasprzyk, A., Keefe, D., Smedley, D., London, D., Spooner, W., Melsopp, C., Hammond, M., Rocca-Serra, P., Cox, T. and Birney, E. (2004) EnsMart: a generic system for fast and flexible access to biological data. *Genome Res.*, **14**, 160–169.

29. Ringwald, M., Eppig, J.T. and Richardson, J.E. (2000) GXD: integrated access to gene expression data for the laboratory mouse. *Trends Genet.*, **16**, 188–190.

30. Halleck, M.S., Lawler, J.J., Blackshaw, S., Gao, L., Nagarajan, P., Hacker, C., Pyle, S., Newman, J.T., Nakanishi, Y., Ando, H. *et al.* (1999) Differential expression of putative transbilayer amphipath transporters. *Physiol. Genomics*, **1**, 139–150.

31. Young, H.M., Bergner, A.J. and Muller, T. (2003) Acquisition of neuronal and glial markers by neural crest-derived cells in the mouse intestine. *J. Comp. Neurol.*, **456**, 1–11.

32. Young, H.M., Ciampoli, D., Hsuan, J. and Canty, A.J. (1999) Expression of Ret-, p75(NTR)-, Phox2a-, Phox2b-, and tyrosine hydroxylase-immunoreactivity by undifferentiated neural crest-derived cells and different classes of enteric neurons in the embryonic mouse gut. *Dev. Dyn.*, **216**, 137–152.

33. Young, H.M., Hearn, C.J., Ciampoli, D., Southwell, B.R., Brunet, J.F. and Newgreen, D.F. (1998) A single rostrocaudal colonization of the rodent intestine by enteric neuron precursors is revealed by the expression of Phox2b, Ret, and p75 and by explants grown under the kidney capsule or in organ culture. *Dev. Biol.*, **202**, 67–84.

34. Pattyn, A., Morin, X., Cremer, H., Goridis, C. and Brunet, J.F. (1999) The homeobox gene Phox2b is essential for the development of autonomic neural crest derivatives. *Nature*, **399**, 366–370.

35. Haddad, G.G., Mazza, N.M., Defendini, R., Blanc, W.A., Driscoll, J.M., Epstein, M.A., Epstein, R.A. and Mellins, R.B. (1978) Congenital failure of automatic control of ventilation, gastrointestinal motility and heart rate. *Medicine*, **57**, 517–526.

36. Matera, I., Bachetti, T., Puppo, F., Di Duca, M., Morandi, F., Casiraghi, G.M., Cilio, M.R., Hennekam, R., Hofstra, R., Schober, J.G. *et al.* (2004) PHOX2B mutations and polyalanine expansions correlate with the severity of the respiratory phenotype and associated symptoms in both congenital and late onset central hypoventilation syndrome. *J. Med. Genet.*, **41**, 373–380.

37. Garcia-Barcelo, M., Sham, M.H., Lui, V.C., Chen, B.L., Ott, J. and Tam, P.K. (2003) Association study of PHOX2B as a candidate gene for Hirschsprung's disease. *Gut*, **52**, 563–567.

38. Kapur, R.P., Yost, C. and Palmiter, R.D. (1992) A transgenic model for studying development of the enteric nervous system in normal and aganglionic mice. *Development*, **116**, 167–175.

39. Britsch, S., Goerich, D.E., Riethmacher, D., Peirano, R.I., Rossner, M., Nave, K.A., Birchmeier, C. and Wegner, M. (2001) The transcription factor Sox10 is a key regulator of peripheral glial development. *Genes Dev.*, **15**, 66–78.

40. Seri, M., Yin, L., Barone, V., Bolino, A., Celli, I., Bocciardi, R., Pasini, B., Ceccherini, I., Lerone, M., Kristoffersson, U. *et al.* (1997) Frequency of RET mutations in long- and short-segment Hirschsprung disease. *Hum. Mutat.*, **9**, 243–249.

41. Maka, M., Stolt, C.C. and Wegner, M. (2005) Identification of *Sox8* as a modifier gene in a mouse model of Hirschsprung disease reveals underlying molecular defect. *Dev. Biol.*, **277**, 155–169.

42. Puffenberger, E.G., Hosoda, K., Washington, S.S., Nakao, K., deWit, D., Yanagisawa, M. and Chakravart, A. (1994) A missense mutation of the endothelin-B receptor gene in multigenic Hirschsprung's disease. *Cell*, **79**, 1257–1266.

43. Mroz, K., Carrel, L. and Hunt, P.A. (1999) Germ cell development in the XXY mouse: evidence that X chromosome reactivation is independent of sexual differentiation. *Dev. Biol.*, **207**, 229–238.

44. Silver, L.M. (1995) *Mouse Genetics, Concepts and Applications.* Oxford University Press, New York, pp. 253–263.

45. Chen, X., Levine, L. and Kwok, P.Y. (1999) Fluorescence polarization in homogeneous nucleic acid analysis. *Genome Res.*, **9**, 492-498.

46. Broman, K.W., Wu, H., Sen, S. and Churchill, G.A. (2003) R/qtl: QTL mapping in experimental crosses. *Bioinformatics*, **19**, 889–890.

47. Churchill, G.A. and Doerge, R.W. (1994) Empirical threshold values for quantitative trait mapping. *Genetics*, **138**, 963–971.

48. Dupuis, J. and Siegmund, D. (1999) Statistical methods for mapping quantitative trait loci from a dense set of markers. *Genetics*, **151**, 373–386.

49. Pletcher, M.T., McClurg, P., Batalov, S., Su, A.I., Barnes, S.W., Lagler, E., Korstanje, R., Wang, X., Nusskern, D., Bogue, M.A. *et al.* (2004) Use of a dense single nucleotide polymorphism map for *in silico* mapping in the mouse. *PLoS Biol.*, **2**, e393.